

## Seismic image segmentation with multiple attributes

Adam D. Halpert\*, Robert G. Clapp, and Biondo Biondi, Stanford University

### SUMMARY

Image segmentation can automatically locate salt boundaries on seismic sections, streamlining an often time-consuming and tedious task when undertaken manually. However, using a single seismic attribute (usually amplitude) is sometimes insufficient to achieve an accurate segmentation result. Since any quantifiable measure may be employed as an attribute for segmentation, it is important to explore other possible attributes in order to develop a more robust segmentation algorithm. Specifically, dip variability and instantaneous frequency attributes show promise for providing unique information relevant to the segmentation problem. Possibilities for combining information from different attributes exist at several different stages of the segmentation process; the most promising methods incorporate an uncertainty measurement that can be easily calculated during segmentation. The ultimate result improves upon single-attribute segmentations by combining the most reliable information from different attributes along different portions of a salt boundary.

### INTRODUCTION

Automated image segmentation offers a means of quickly and efficiently delineating salt bodies on seismic images. When adapted for seismic purposes (Lomask, 2007; Lomask et al., 2007), the Normalized Cuts Image Segmentation (NCIS) algorithm (Shi and Malik, 2000) provides a global solution to the salt boundary calculation. This helps overcome some of the weaknesses of other methods, such as local horizon trackers, that can fail when the boundary fades or becomes discontinuous. A global determination of salt boundaries can be especially important for building velocity models in complex areas; in such cases, image segmentation may be employed to automatically build or update velocity models, helping to alleviate a major bottleneck for iterative imaging projects (Halpert et al., 2008).

The segmentation algorithm relies on one or more seismic attributes to segment an image; the most straightforward of these attributes is amplitude of the envelope. Often, this single attribute provides an accurate calculation of the salt boundary. Unfortunately, in some instances a single attribute is insufficient, and the algorithm cannot produce a reasonable result. Here, we explore two possibilities for useful attributes other than amplitude: dip variability and instantaneous frequency. We demonstrate that these attributes are indeed viable for segmentation, and proceed to explore possibilities for combining information from these different attributes. Using a 2D seismic section from a field dataset as an example, we show that combining two attributes (amplitude and dip variability) via a mechanism that takes into account uncertainties at each boundary location provides a result superior to those using only a single segmentation attribute.

#### Segmentation process

The NCIS algorithm for seismic image segmentation functions by determining the likelihood of a salt interface existing between individual pixel pairs in an image, and using this information to calculate an eigenvector of the image (for details, see Lomask et al. (2007)). Values of the eigenvector range from -1 to +1 across a potential boundary; usually, following the zero-contour of the eigenvector will yield the most appropriate boundary choice for the image. However, when the transition from positive to negative eigenvector values across the boundary is very slow (illustrated by extended “gray areas” in depictions of an eigenvector such as those in Figure 5), the location of the boundary is much more uncertain than in the case of a faster and sharper transition. This concept provides

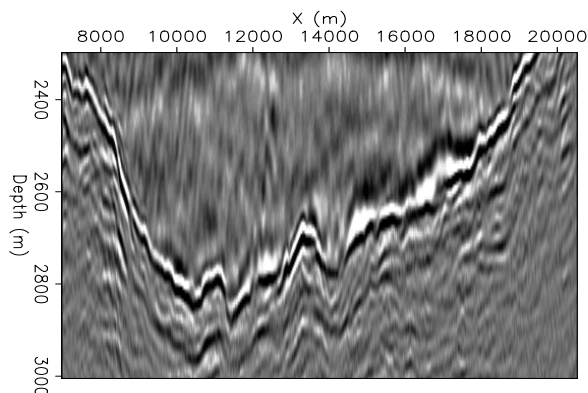


Figure 1: A migrated 2D seismic image used to demonstrate attribute calculations.

important information for the attribute combination scheme we will detail here. It is important to note that while the examples provided here are in 2D, the segmentation process is extendable to 3D; presumably, a three-dimensional case would exhibit less uncertainty around the boundary due to a far larger number of pixel-to-pixel comparisons.

### SEGMENTATION ATTRIBUTES

In order to calculate the likelihood of a salt interface existing between two pixels of a migrated seismic image such as in Figure 1, the segmentation algorithm uses attribute information gleaned from the image. The most common and intuitive attribute used for this purpose is amplitude of the envelope. For instance, a large amplitude between two pixels suggests a salt boundary is likely, while the absence of a large amplitude value indicates that a boundary is unlikely. Panel (a) in Figure 2 shows this attribute calculated for the seismic image in Figure 1; the salt boundary is clearly identifiable. Amplitude, however, is not the only attribute that can be used for this purpose. In fact, any quantifiable measure that relates to the presence of a salt boundary may be used as an attribute for segmentation. It stands to reason that these other attributes will be most useful in areas of the subsurface characterized by unreliable or missing amplitude information, perhaps as a result of poor illumination.

#### Dip variability

Estimating dip in seismic images has long been recognized as a useful interpretation technique, especially for 3D volumes (Bednar, 1998). Dip can be a particularly useful attribute when the goal is delineation of salt bodies. Lomask (2007) notes that salt boundaries and nearby sediments will often display different dips; furthermore, the seemingly random dips that often characterize the interior of salt bodies on field seismic data should contrast considerably with more ordered dipping layers outside the salt. Therefore, an attribute that highlights variability in dip throughout a seismic image may be helpful for locating salt boundaries.

Dips on seismic images may be estimated in several ways. Here, we use a “plane-wave destructor” method with a filter proposed by Hale (2007) that was designed to function even at very steep dips; filters developed by Claerbout (1992) and Fomel (2002) are also possibilities. To highlight changes in the dip (an abrupt change

## Segmentation with multiple attributes

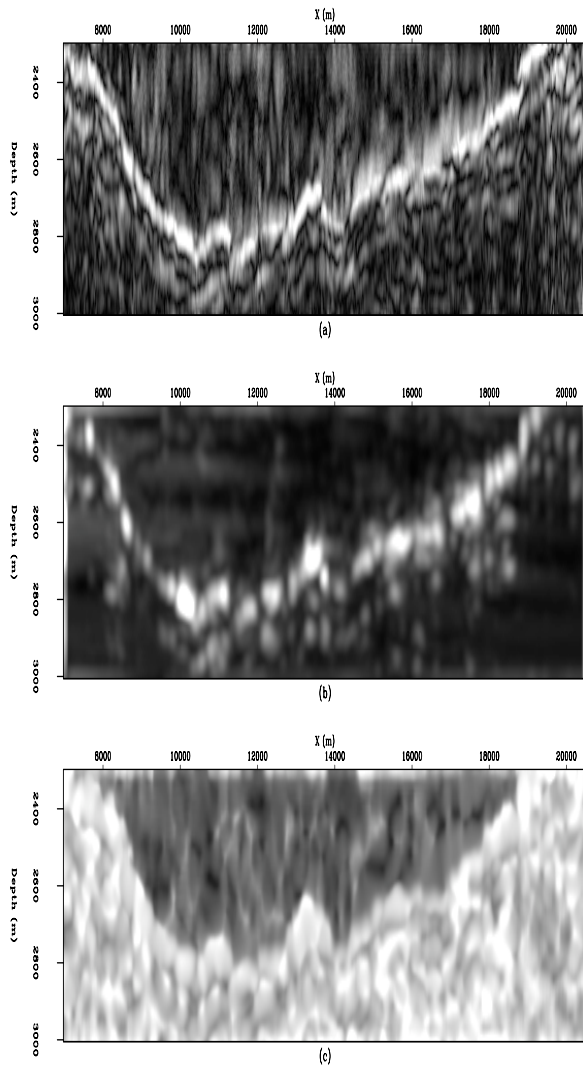


Figure 2: Amplitude (a), dip variability (b), and instantaneous frequency (c) calculations used as inputs to the segmentation process.

is indicative of a salt boundary), a roughener should be applied; here, the helical derivative (Claerbout, 2005) is used to facilitate extension to three dimensions. Finally, calculating the envelope of this volume will produce an image suitable for the segmentation process. Panel (b) in Figure 2 shows the dip variability calculation applied to the image in Figure 1.

### Instantaneous frequency

Seismic waves behave differently inside salt bodies than they do when traveling through sediment layers. One way to take advantage of this fact is to calculate *instantaneous frequency* (Taner et al., 1979) in different parts of an image. In the complex representation of a seismic trace

$$A(t)e^{i\phi(t)}, \quad (1)$$

$A(t)$  is the amplitude of the envelope (the most common segmentation attribute), and  $\phi(t)$  is the instantaneous phase. The first derivative of the instantaneous phase yields instantaneous frequency. A rapid change in instantaneous frequency may be indicative of a salt boundary, especially if it occurs in a coherent manner across an image. Panel (c) in Figure 2 shows the instantaneous frequency

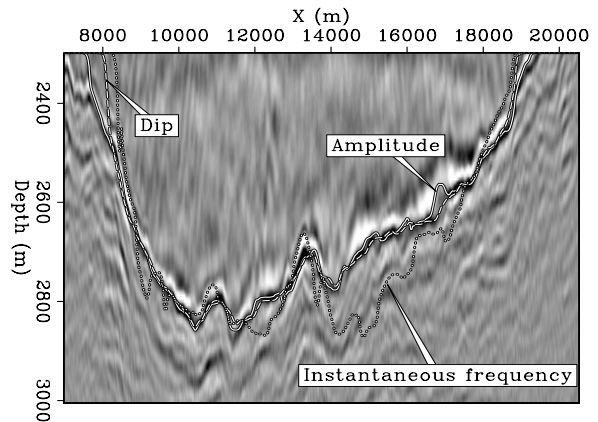


Figure 3: Boundaries corresponding to the amplitude, dip variability and instantaneous frequency calculations seen in Figure 2.

calculation for the same 2D section used previously. It is apparent that frequency behavior inside the salt differs noticeably from behavior outside the salt.

### COMBINING ATTRIBUTE INFORMATION

Figure 3 displays the zero-contour boundaries corresponding to the three attribute volumes shown in Figure 2. Clearly, each of the three attributes provides differing information on the exact location of the salt boundary. The next step is to find a way to combine this information into a single segmentation result that incorporates the best information provided by each attribute.

In the segmentation algorithm, the determination of a salt interface takes place in three distinct stages. The first stage is the calculation of attributes that may be useful in indicating a boundary between sediments and a salt body. The second stage involves transforming the attribute volumes into eigenvectors of the image via the construction of a weight matrix based on the attribute values. Finally, the third stage “draws” the salt boundary using the eigenvector values. Each of these three stages represents an opportunity for combining information from different attributes. The following sections will explore these three options, and illustrate their advantages and disadvantages with example calculations on another 2D seismic section taken from a 3D Gulf of Mexico field dataset, seen in Figure 4.

The following examples will seek to combine useful information from two attributes - amplitude and dip variability. Figure 5 shows eigenvectors derived from these two individual attributes. Recall that a sharp transition from dark to light colors in the eigenvector indicates a boundary location with relative certainty, while a gray area indicates a slower transition and relative uncertainty of the boundary location. Clearly, the amplitude eigenvector provides better information throughout most of the image, although the transition near  $x = 18000$  suggests significant uncertainty. This is logical, as the original section (Figure 4) shows a great deal of discontinuity at this location. Overall, the dip eigenvector shows much less certainty than the one derived from the amplitude attribute; however, the previously mentioned location appears more certain on the dip eigenvector. The boundary calculations corresponding to these two eigenvectors (Figure 6) confirm these observations. Therefore, an obvious goal for combining information from these two attributes is to produce a boundary that uses information from the amplitude attribute in most locations, but incorporates the dip information at this location.

## Segmentation with multiple attributes

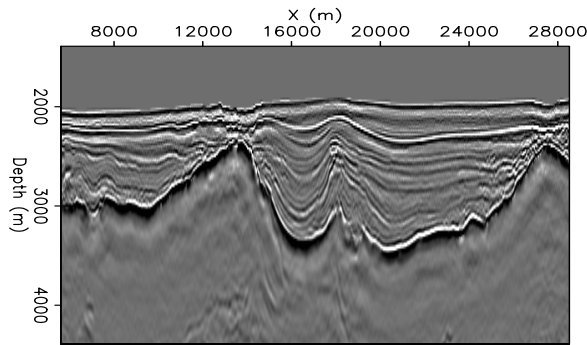


Figure 4: A migrated seismic section used for examples throughout this paper. Note the discontinuous nature of the strong reflector (salt boundary), which will present challenges for the segmentation algorithm.

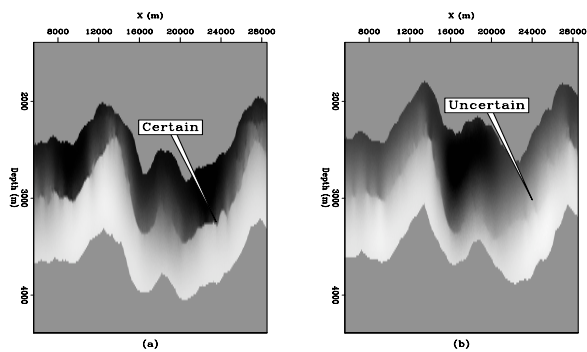


Figure 5: Eigenvectors derived from amplitude of the envelope (a) and dip variability (b) attributes. Areas of relative boundary certainty and uncertainty are indicated.

### Attribute multiplication

One approach, suggested by Lomask (2007), is to combine multiple attribute volumes into a single volume via multiplication:

$$A = \prod_{i=\text{all attributes}} a_i, \quad (2)$$

where  $a$  is an individual attribute volume, and then proceed with segmentation normally. Multiplication of the attribute data has the effect of reinforcing information in areas where the attributes “agree,” which can be beneficial. However, it also can have the effect of destroying potentially valuable information if the two attributes are not in agreement. Panel (a) in Figure 7 shows the boundary calculation resulting from this process. Clearly, in this case the disadvantages of multiplying attribute volumes together outweigh the possible advantages - the process appears to have incorporated the worst information from each of the attributes, resulting in a final boundary that does not improve on either of the individual results (Figure 6) in any location.

### Boundary combinations

A second “domain” in which information from different attributes may be combined is after individual boundary calculations have already taken place. This method requires a measure of uncertainty along each individual boundary, so that a new boundary can be created by incorporating the “most certain” boundary at each location in the image. As discussed previously, such an uncertainty measure

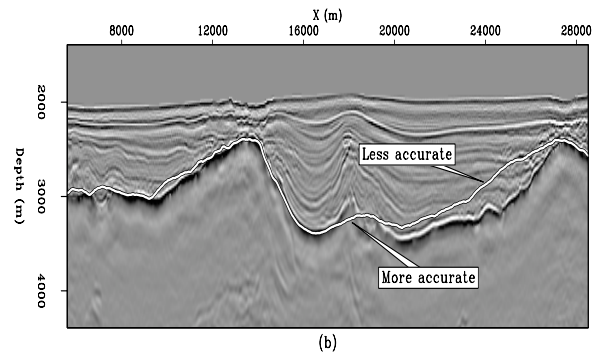
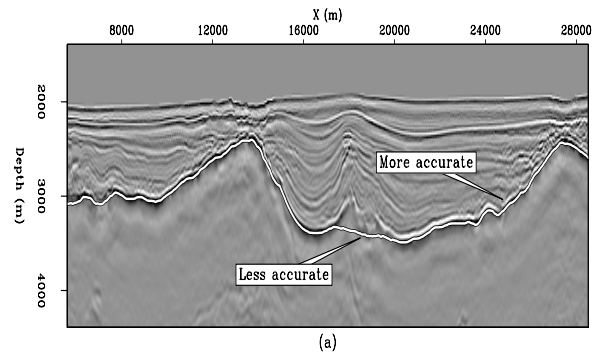


Figure 6: Zero-contour boundaries corresponding to the amplitude (a) and dip variability (b) eigenvectors seen in Figure 5.

may be gleaned from the zero-crossing of the eigenvector:

$$d = |p_1 - n_1|, \quad (3)$$

where  $p_1$  and  $n_1$  are the two values on either side of the boundary (one will be positive, one negative). A sharp transition from positive to negative values - quantitatively, a large value of  $d$  at that location - signifies relative certainty, while a slow transition or small difference signals uncertainty. In this case, the measurement is taken perpendicular to the calculated boundary, so as to avoid the assumption that the boundary is in all locations locally horizontal. After such calculations are made at all locations for each boundary, a combined boundary is formed by taking the most certain boundary location (depth value) at each horizontal location. Panel (b) in Figure 7 shows the result of this process.

This approach performs very well in this example. Information from the amplitude attribute is honored nearly everywhere, and the dip information is incorporated only where it is superior to the amplitude information. However, the manner in which this approach is implemented could lead to problems in some circumstances. Taking the best elements of different boundaries could easily lead to erratic, “either/or” behavior in the combined boundary; indeed, some indications of this behavior may be seen in the jaggedness of the boundary where the dip information plays a significant role. It is likely that this behavior would be even more troublesome in three dimensions.

### Eigenvector combinations

Finally, a third approach is to use the individual attribute volumes to calculate multiple eigenvectors, and then combine the eigenvectors before determining a boundary. Following the recommendation of Shi and Malik (2000), a simple way to combine the eigenvectors is via linear combination:

## Segmentation with multiple attributes

$$E = \sum_{i=\text{all attributes}} \lambda_i e_i, \quad (4)$$

where  $e$  is an individual eigenvector and  $\lambda$  is a specific weight value assigned to the attribute in question. Of course, taking this approach introduces the problem of determining weight values for each attribute. Panel (c) in Figure 7 shows the result of this approach if equal weights are given to the amplitude and dip attributes. While the boundary is satisfactory in many locations, the dip attribute clearly has too much influence in some areas where the amplitude attribute provides much better information. This method shows promise, but a mechanism for assigning better weights is necessary. One such mechanism has already been discussed; we can use the eigenvector uncertainty measurement, utilized previously for the boundary combination approach, to assign attribute weight values for a linear combination of eigenvectors. In this way, we are able to follow the recommendation of Shi and Malik for combining information from different sources, while at the same time taking advantage of a “built-in” method for estimating uncertainties.

Since the eigenvectors range in value from -1 to +1, the eigenvector difference across one of the boundaries can never be greater than two. Thus, the value

$$\omega = \frac{1}{2}(d_{amp} - d_{dip}), \quad (5)$$

where  $d$  is the difference across a calculated boundary at a particular  $x$  location, will range from 0 to 1. If we want to heavily penalize uncertainty in one of the eigenvectors, we set the weight values as follows:

$$W_{amp} = \begin{cases} \omega^2 & \text{if } \omega < 0.5 \\ \sqrt{\omega} & \text{if } \omega > 0.5 \end{cases} \quad (6)$$

$$W_{dip} = 1 - w_{amp}. \quad (7)$$

The results of assigning weight values in this manner to create an eigenvector are shown in panel (d) of Figure 7. The boundary successfully follows the salt interface everywhere the amplitude-only boundary does, and incorporates the dip information only where the amplitude boundary fails. Furthermore, we do not see the erratic behavior in areas where the dip information is most significant, as we did for the boundary combination method.

### CONCLUSIONS

Automatic image segmentation has the potential to offer interpreters a quick and efficient means of delineating salt boundaries on seismic images. Since using amplitude information alone is sometimes insufficient to produce an accurate boundary calculation, other attributes such as dip variability and instantaneous frequency may also be used successfully. By combining information from different attributes, we hope to incorporate the most reliable information from each attribute into a single, improved segmentation result. While opportunities for such combinations exist at several stages of the segmentation process, the most promising method involves a linear combination of eigenvectors from individual attributes, weighted according to uncertainties derived from each eigenvector. In the examples here, such an approach successfully incorporates useful information from two different attributes, while avoiding potential pitfalls of other methods.

### ACKNOWLEDGMENTS

We would like to thank WesternGeco and Phil Schultz (formerly at Unocal, now Chevron) for providing the field data used in these examples, and the sponsors of the Stanford Exploration Project for their support.

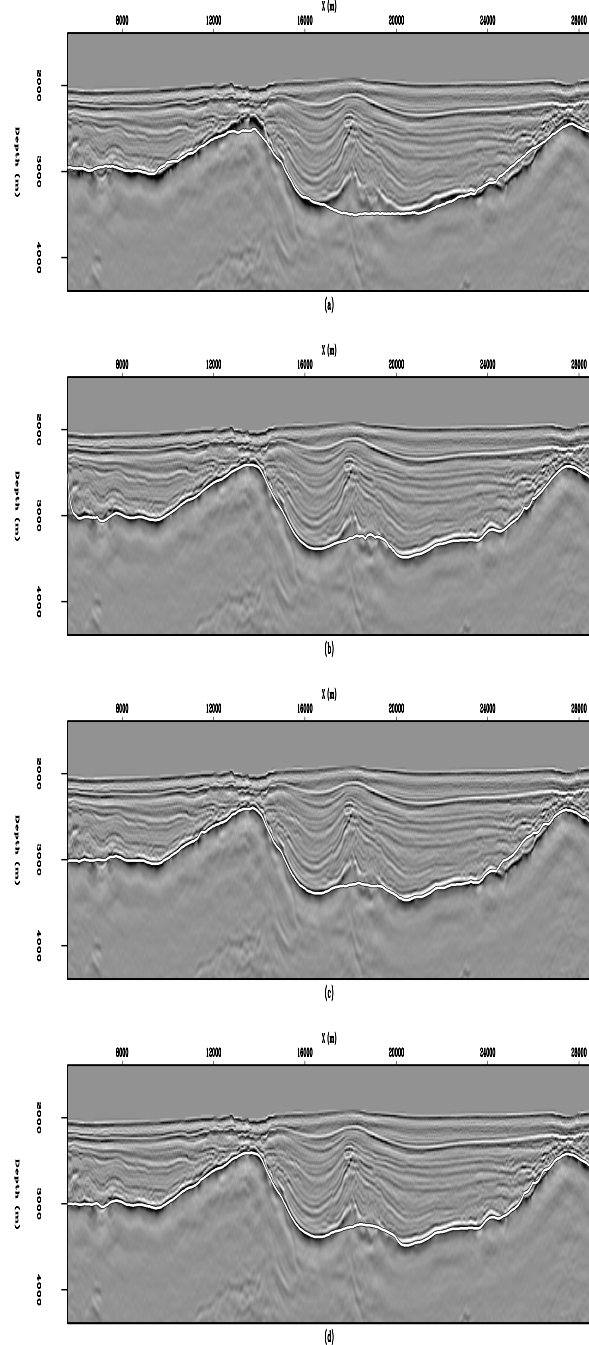


Figure 7: Calculated boundaries corresponding to: (a) Attribute multiplication segmentation; (b) Combination of individual boundaries; (c) Equally-weighted eigenvector combination; and (d) Uncertainty-weighted eigenvector combination.

## EDITED REFERENCES

Note: This reference list is a copy-edited version of the reference list submitted by the author. Reference lists for the 2009 SEG Technical Program Expanded Abstracts have been copy edited so that references provided with the online metadata for each paper will achieve a high degree of linking to cited sources that appear on the Web.

## REFERENCES

- Bednar, J. B., 1998, Least squares dip and coherency attributes: *The Leading Edge*, **17**, 775–776.
- Claerbout, J., 1992, *Earth soundings analysis: Processing versus inversion*: Blackwell Scientific Publications.
- Claerbout, J., 2005, *Image estimation by example*: Stanford University.
- Fomel, S., 2002, Applications of plane-wave destruction filters: *Geophysics*, **67**, 1946–1960.
- Hale, D., 2007, Local dip filtering with directional laplacians: *CWP Report*, 567, 1–12.
- Halpert, A., R. G. Clapp, J. Lomask, and B. L. Biondi, 2008, Image segmentation for velocity model construction and updating: 78th Annual International Meeting, SEG, Expanded Abstracts, 3088–3092.
- Lomask, J., R. G. Clapp, and B. Biondi, 2007, Application of image segmentation to tracking 3D salt boundaries: *Geophysics*, **72**, P47–P56.
- Lomask, J., 2007, *Seismic volumetric flattening and segmentation*: Ph. D. thesis, Stanford University.
- Shi, J. and J. Malik, 2000, Normalized cuts and image segmentation: *Institute of Electrical and Electronics Engineers Transactions on Pattern Analysis and Machine Intelligence*, 22, 838–905.
- Taner, M. T., F. Koehler, and R. E. Sheriff, 1979, Complex seismic trace analysis: *Geophysics*, **44**, 1041–1063.